DEUTSCHES ELEKTRONEN-SYNCHROTRON DESY

DESY 74/40
August 1974

$\Delta^{++}\pi^{-}$-Electroproduction Near Threshold and the Q^2 Dependence of the Contact Interaction

by

P. Joos, A. Ladage, H. Meyer, D. Notz, P. Stein, G. Wolf and S. Yellin
Deutsches Elektronen-Synchrotron DESY, Hamburg

C. Benz, G. Drews, D. Hoffmann, J. Knobloch, W. Kraus, H. Nagel, E. Rabe, C. Sander, W.-D. Schlatter, H. Spitzer, K. Wacker and P. Winkler
II. Institut für Experimentalphysik der Universität Hamburg

I. J. Bloodworth, C. K. Chen, J. Knowles, D. Martin, J. M. Scarr, I. O. Skillicorn and K. Smith
University of Glasgow, Glasgow

2 HAMBURG 52 · NOTKESTIEG 1

To be sure that your preprints are promptly included in the
HIGH ENERGY PHYSICS INDEX ,
send them to the following address (if possible by air mail) :

DESY
Bibliothek
2 Hamburg 52
Notkestieg 1
Germany

$\Delta^{++}\pi^{-}$-Electroproduction near Threshold and the Q^2 Dependence of the Contact Interaction

P. Joos, A. Ladage, H. Meyer, D. Notz*, P. Stein**, G. Wolf, and S. Yellin***
Deutsches Elektronen-Synchrotron DESY, Hamburg

C. Benz, G. Drews, D. Hoffmann, J. Knobloch, W. Kraus, H. Nagel, E. Rabe, C. Sander, W.-D. Schlatter, H. Spitzer, K. Wacker, and P. Winkler
II. Institut für Experimentalphysik der Universität Hamburg

I.J. Bloodworth, C.K. Chen, J. Knowles, D. Martin, J.M. Scarr, I.O. Skillicorn, and K. Smith
University of Glasgow, Glasgow

Abstract: The Q^2 dependence of $\sigma(\gamma_V p \to \pi^- \Delta^{++})$ was measured. Close to threshold $\sigma(\gamma_V p \to \pi^- \Delta^{++})$ is roughly proportional to $1/(m_\rho^2 + Q^2)^2$. The data are consistent with dominance of the contact term and imply that the contact term has the Q^2 dependence of the ρ propagator.

Photo- and electroproduction near threshold of the $\Delta(1236)$ via

$$\gamma_V p \to \pi^- \Delta^{++} \qquad (1)$$

provides a unique opportunity of studying experimentally the properties of the $\gamma N\pi\Delta$ contact term. The existence of a large contact interaction in reaction (1) was first proposed by Cutcosky and Zachariasen[1] in a static model. In the model of Stichel and Scholz[2] for reaction (1) the contact term is a gauge correction for the one-pion exchange and dominates in the threshold region. Lüke and Söding[3], in a detailed analysis of the photoproduction data of the ABBHHM collaboration[4] have demonstrated that within the existing models the qualitative features of reaction (1) near threshold, namely the isotropic production, the rapid rise of the cross section and its magnitude near threshold could only be understood as a consequence of the contact term. An important question is the Q^2 behaviour of the contact term. For instance in the case of e^+e^- annihilation into hadrons it is speculated that the major part of the cross section comes from pointlike γ-three hadron contact terms[5]. The assumption of pointlike behaviour is here the necessary ingredient to get a large cross section.

* Now at CERN, Geneva
** On leave of absence from Cornell University, Ithaca, NY, USA
*** Now at University of California, Santa Barbara, California, USA

The Q^2 dependence of reaction (1) in the space-like region can be studied in an electroproduction experiment. The linear polarization of the transverse photons permits an even better test of the contact term than is possible with photoproduction by unpolarized photons. For instance, the contact interaction is independent of the transverse photon polarization while one-pion exchange is not.

We have, for the first time, measured reaction (1) in the threshold region for Q^2 values between 0.3 and 1.5 GeV^2 in an attempt to extract the properties of the contact term.

Experimental setup and analysis procedure: The experiment uses a 7.2 GeV electron beam from the DESY synchrotron and a 1m streamer chamber. The chamber is inside a 18 kG magnet. The electron beam strikes a liquid hydrogen target inside the chamber. A counter hodoscope consisting of scintillation and shower counters, and proportional chambers detects the scattered electron and triggers the chamber. The produced hadrons are detected in the full solid angle. The analysis of the photographs is similar to that of bubble chamber film. Details of the setup, the analysis procedures and first results from smaller samples of data can be found elsewhere[6,7].

The present analysis is based on approximately one third of the total exposure. In total 4029 events of the type

$$ep \rightarrow ep\pi^+\pi^- \tag{2}$$

were found with Q^2 between 0.3 and 1.5 GeV^2 and the total hadron energy, W, in the region $1.3 < W < 2.8$ GeV. The data presented below is mainly from the threshold region ($1.3 < W < 1.5$ GeV) where the contact term is strongest.

Δ^{++} production: The $p\pi^+$, $p\pi^-$ and $\pi^+\pi^-$ mass distributions are shown in Fig. 1. The cross sections for Δ^{++}, and Δ^o production were determined by a maximum-likelihood fit to the Dalitz plot density $dN(M^2_{p\pi^+}, M^2_{\pi^+\pi^-})$:

$$dN(M^2_{p\pi^+}, M^2_{\pi^+\pi^-}) = \Big[a_{\Delta^{++}} f_{\Delta^{++}} (M_{p\pi^+}) + a_{\Delta^o} f_{\Delta^o} (M_{p\pi^-}) + a_{ps} f_{ps} \Big] dM^2_{p\pi^+} dM^2_{\pi^+\pi^-} \tag{3}$$

The a's are fit parameters and measure the size of the individual contributions; $f_{\Delta^{++}}$ and $f_{\Delta^{o}}$ represent the corresponding Breit-Wigner terms. For $W > 1.7$ GeV an appropriate term was added describing ρ production[6]. The lines in Fig. 1 give the results of the fit. The fit shows that Δ^{++} production dominates.

Figs. 2 and 3 show the W and Q^2 dependence of the Δ^{++} cross section. When averaged over Q^2 the Δ^{++} cross section shows an energy dependence similar to that found in photoproduction[3,4], namely a sharp rise above threshold to a peak at ~1.6 GeV followed by a steady fall with energy. Fig.4 shows the characteristics of the angular distributions in the threshold region. The production angular distribution $d\sigma/d\cos\Theta^*$, determined from a maximum likelihood fit in various $\cos\Theta^*$ intervals, is shown in Fig. 4e. It is approximately constant which is consistent with dominant s-wave production. The Δ^{++} density matrix elements[6,8] were determined by the method of moments as a function of $\cos\Theta^*$. Fig. 4(a)-(d) shows four of the 16 matrix elements measured in this experiment. The r^{o4}_{ik} matrix elements were determined in the Gottfried-Jackson frame for $1.3 < W < 1.5$ GeV; only the r^{o4}_{11} and r^{o4}_{33} matrix elements are different from zero. The r^1, r^2, r^5 and r^6 matrix elements (not shown) are all consistent with zero[9]. The relative amounts of natural to unnatural parity exchange is measured by the trace of r^1 (see refs. 6, 8); within errors the trace is zero at all W's; hence approximately equal contributions of natural and unnatural parity exchanges are present. The fact that the matrices r^5 and r^6 are zero implies that the longitudinal-transverse interferences are small.

In photoproduction the sharp rise of the $\pi^-\Delta^{++}$ cross section above threshold can be explained quantitatively by the onset of the contact interaction[2] (diagram (a) of Fig. 5). The contact term is one of four electric Born diagrams which constitute the gauge invariant one pion exchange model of Stichel and Scholz[2]. At low W the contact term dominates, while at high energies the other terms become important. When absorption corrections are applied fair agreement is found even at high energies[4,10].

The model was extended to electroproduction by Bartl et al.[11]. The differential cross section for $\pi^-\Delta^{++}$ production by virtual transverse (T) and longitudinal (L) photons, respectively, is given in the Born approximation by:

$$\frac{d\sigma}{dt}^{(T)}_{(L)} = \frac{1}{128\pi\, q_\gamma^2\, W^2}\ \frac{\alpha/4}{\gamma_\rho^2/4\pi} \times \begin{cases} \sum_{\lambda_\Delta,\lambda_p,\lambda_\gamma=\pm 1} |f^V_{\lambda_\Delta,\lambda_p,\lambda_\gamma}|^2 \\ 2\sum_{\lambda_\Delta,\lambda_p,0} |f^V_{\lambda_\Delta,\lambda_p,0}|^2 \end{cases} \qquad (3)$$

where $t = (p-\Delta)^2$, q_γ = photon momentum in the hadron cms, $\alpha = 1/137$, $\gamma_\rho^2/4\pi = 0.6$; the helicity amplitudes $f^V_{\lambda_\Delta,\lambda_p,\lambda_\gamma}$ can be found in Ref. 11. The Q^2 dependence of $d\sigma^T/dt$ is essentially determined by the flux factor $(q_\gamma^2\, W^2)^{-1} = (W^2 - Q^2 - m_p^2)^2/4 + W^2\, Q^2$. For $Q^2 < 1$ GeV^2 $\sigma^L << \sigma^T$.

According to the model, the dominant mechanism for Δ^{++} production by transverse photons near threshold is the contact term as in photoproduction. Qualitatively the contact term leads to: a rapid rise of $\sigma(\pi^-\Delta^{++})$ above threshold, an isotropic production angular distribution, and equal amounts of natural and unnatural parity exchange in the t channel, i.e. $r^1_{11} + r^1_{00} = 0$. These features are consistent with the data. Additionally, the density matrix elements predicted by the model agree with the data (see Fig. 4). Thus we conclude that all aspects of the data are consistent with the dominance of the contact term at threshold.

We now determine the Q^2 dependence of the contact term for all momentum transfers and for small t-values ($|t| < 0.7$ GeV^2)*. The latter restriction is suggested by the model which predicts that at large momentum transfers there is some contribution from u-channel Δ exchange to the longitudinal cross section. In Fig. 3 the measured values of $\sigma(\pi^-\Delta^{++})$ are compared with the Born cross section calculated from eq.(3) (dashed curve) as a function of Q^2. The data clearly fall off more rapidly than the theoretical curves being low by a factor of 4 at $Q^2 = 0.6$ GeV^2. We therefore multiplied the Born amplitudes by a common factor $(1 + Q^2/m^2)^{-1}$ and fitted the data for m allowing for an arbitrary normalisation constant. The fit gives $m = 0.89 \pm 0.1$ GeV,

* The theoretical cross sections were calculated as an average over the same Q^2,W region as that used for the data points. The averaging procedure included weigthing by the virtual photon flux in order to represent the procedure applied to the data.

which is consistent with the rho mass. From this we conclude that the contact term falls with Q^2 like the rho propagator as would be suggested by VDM. The solid curves in Figs. 2-4 give the prediction of the model including the rho propagator; all predictions are in reasonable agreement with the data.

In summary, we find, that after dividing out the photon flux factor (q_γ in eq.(3)), $\sigma(\pi^- \Delta^{++})$ near threshold is proportional to $(m_\rho^2 + Q^2)^{-2}$. Further, the qualitative features as well as the size of the cross section observed in this experiment agree with the assumption that the threshold region is dominated by the contact term, in accord with the Stichel-Scholz model. Under this assumption, then, we conclude that the contact term has the Q^2 dependence of the ρ propagator.

One of us (G. W.) wants to thank Prof. A. Bartl for a clarifying correspondence. The work at Hamburg has been supported by the Bundesministerium für Forschung und Technologie.

References

1. R.E. Cutcosky and F. Zachariasen, Phys. Rev. 103, 1108 (1956)
2. P. Stichel and M. Scholz, Nuovo Cimento 34, 1381 (1964)
3. D. Lüke and P. Söding, Springer-Tracts in Modern Physics, 59, 39 (1971)

   D. Lüke, Ph.D. Thesis, Internal Report DESY F1-72/7 (1972)
4. Aachen-Berlin-Bonn-Hamburg-Heidelberg-München-Collaboration, Phys. Rev. 175, 1669 (1968)
5. C. Ferro Fontan and H.R. Rubinstein, CERN TH-1810 (1974)
6. V. Eckardt et al., Nucl. Phys. B55, 45 (1973)
7. V. Eckardt et al., DESY 74/5 (1974)
8. K. Schilling and G. Wolf, Nucl. Phys. B61, 381 (1973)
9. E. Rabe, DESY Internal Report F1-74/2 (1974)
10. J. Ballam et al., Phys. Rev. D5, 545 (1972)
11. A. Bartl, W. Majerotto and D. Schildknecht, Nuovo Cimento 12A, 703 (1972)
12. M.P. Locher and W. Sandhas, Z. Physik 195, 461 (1966)

Figure Captions

Fig. 1 $M_{p\pi^+}$, $M_{p\pi^-}$ and $M_{\pi^+\pi^-}$ distributions for $1.3 < W < 1.5$ GeV and three Q^2 intervals. The curves are from the Dalitz plot fit.

Fig. 2 $\sigma(\gamma_V p \to \pi^- \Delta^{++})$ as a function of W for $0.3 < Q^2 < 1.5$ GeV^2 and $|t| < 0.7$ GeV^2. The curves are predictions of the Born term model modified by vector dominance. The dashed curve includes absorption corrections.

Fig. 3 $\sigma(\gamma_V p \to \pi^- \Delta^{++})$ for $1.3 < W < 1.5$ GeV as a function of Q^2. (a) no t cut, (b) for $|t| < 0.7$ GeV^2. The curves are predictions of the Born term model with (——) and without (- - -) the ρ propagator factor. $\bar{\rho}$ is the photoproduction value from Ref. 4.

Fig. 4(a)-(d) Density matrix elements r^{04}_{ik} in the Δ^{++} region ($1.12 < M_{p\pi^+} < 1.32$ GeV in the Gottfried-Jackson-System as a function of $\cos\Theta^*$ (Θ^* is the cms production angle of the Δ^{++}) for $0.3 < Q^2 < 1.5$ GeV^2. The curves are predictions of the Born term model modified by vector dominance.
(e) $d\sigma/d\cos\Theta^*$ for the reaction $\gamma_V p \to \pi^- \Delta^{++}$. The cross sections were obtained by maximum likelihood fits to the Dalitz plot in $\cos\Theta^*$ intervals. The curve is from the Born term model modified by vector dominance.

Fig. 5(a)-(d) Born terms used to describe $\gamma_V p \to \pi^- \Delta^{++}$ in the model of Stichel and Scholz.

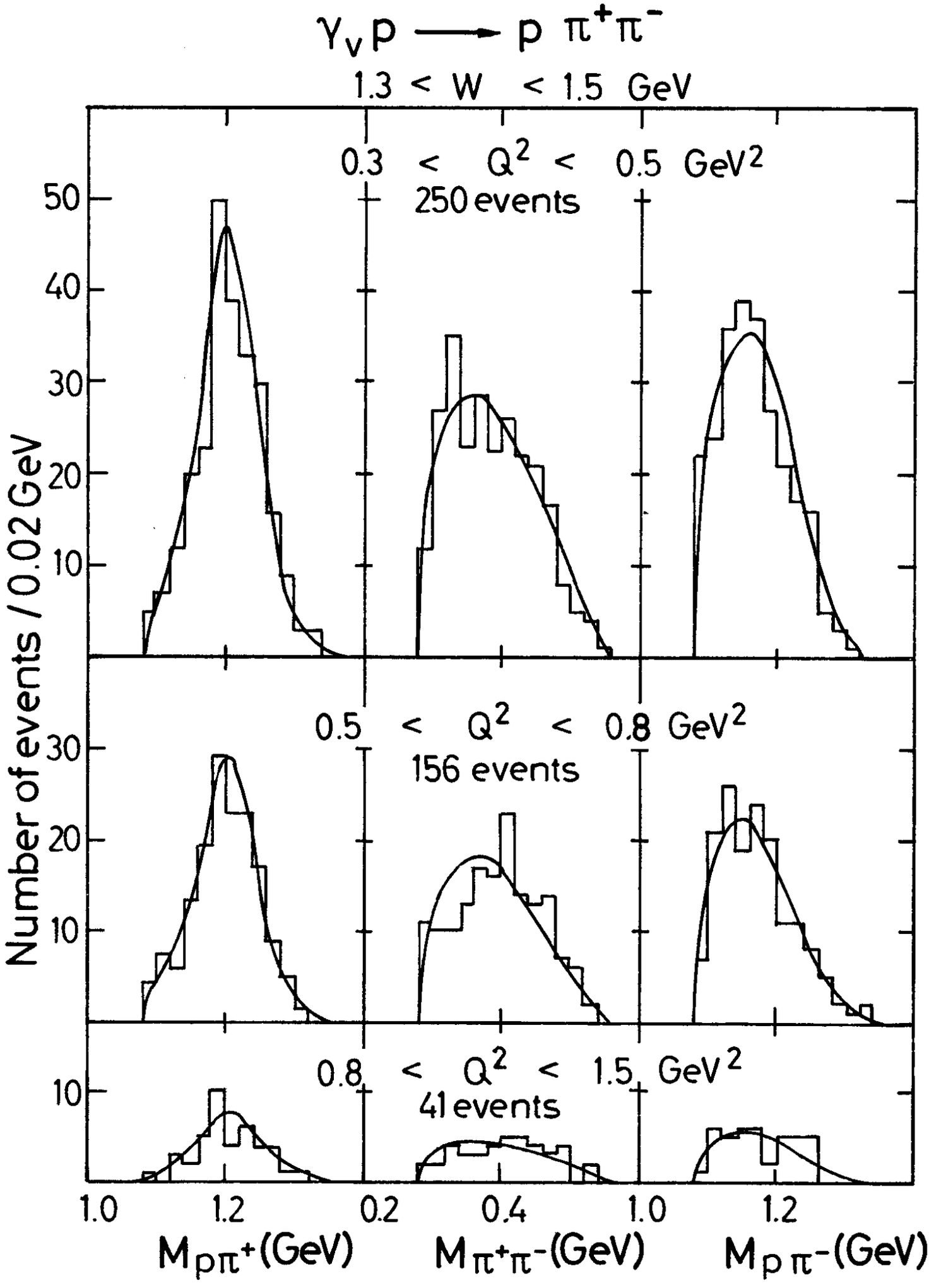
$\gamma_v p \longrightarrow p\ \pi^+\pi^-$
1.3 < W < 1.5 GeV
0.3 < Q² < 0.5 GeV²
250 events
0.5 < Q² < 0.8 GeV²
156 events
0.8 < Q² < 1.5 GeV²
41 events
Number of events / 0.02 GeV
50
40
30
20
10
30
20
10
10
1.0
1.2
0.2
0.4
1.0
1.2
$M_{p\pi^+}$(GeV)
$M_{\pi^+\pi^-}$(GeV)
$M_{p\pi^-}$(GeV)

Fig.1

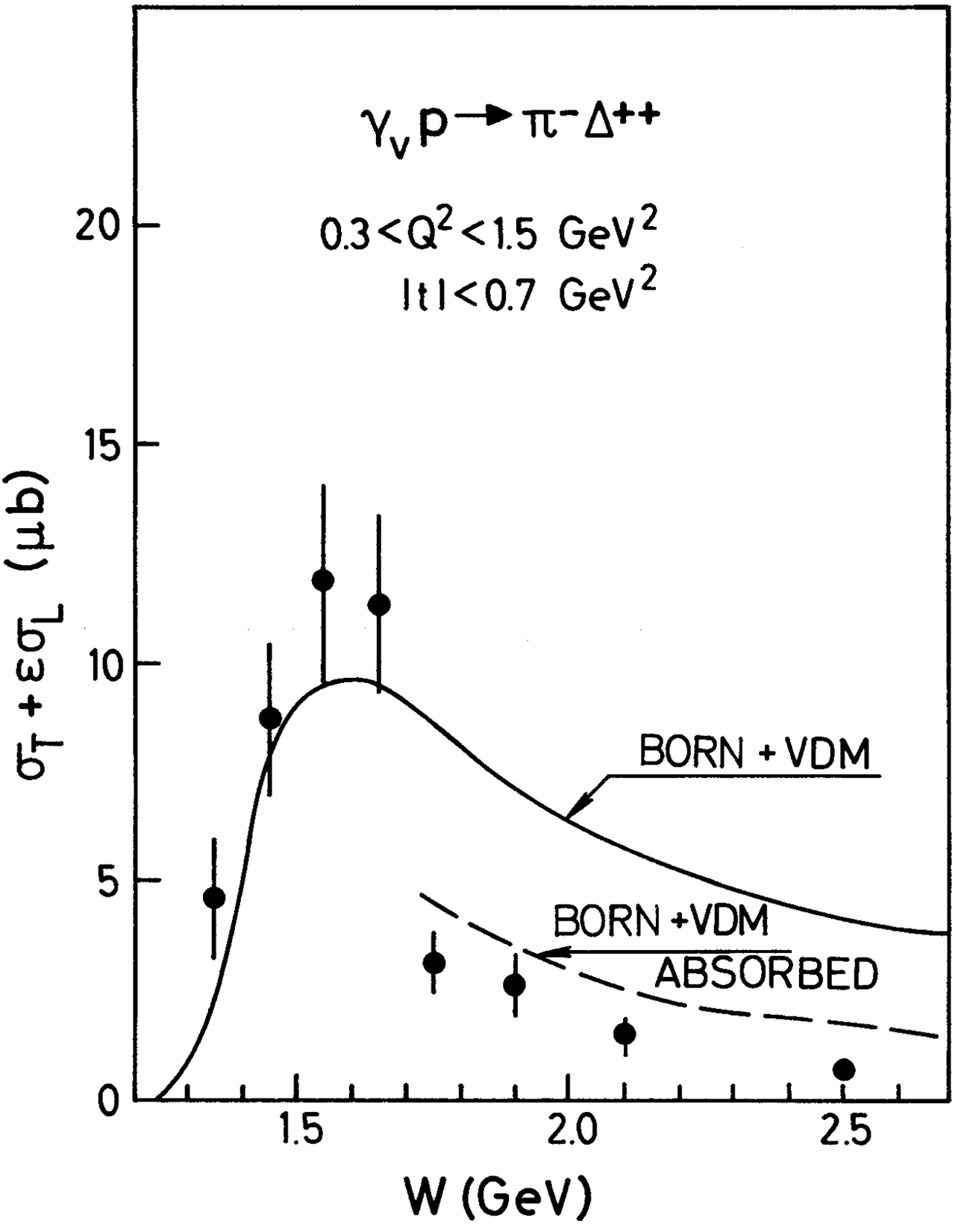
$\gamma_v p \rightarrow \pi^- \Delta^{++}$
$0.3 < Q^2 < 1.5$ GeV^2
$|t| < 0.7$ GeV^2
$\sigma_T + \varepsilon\sigma_L$ (μb)
BORN + VDM
BORN + VDM
ABSORBED
W (GeV)
0
5
10
15
20
1.5
2.0
2.5

Fig.2

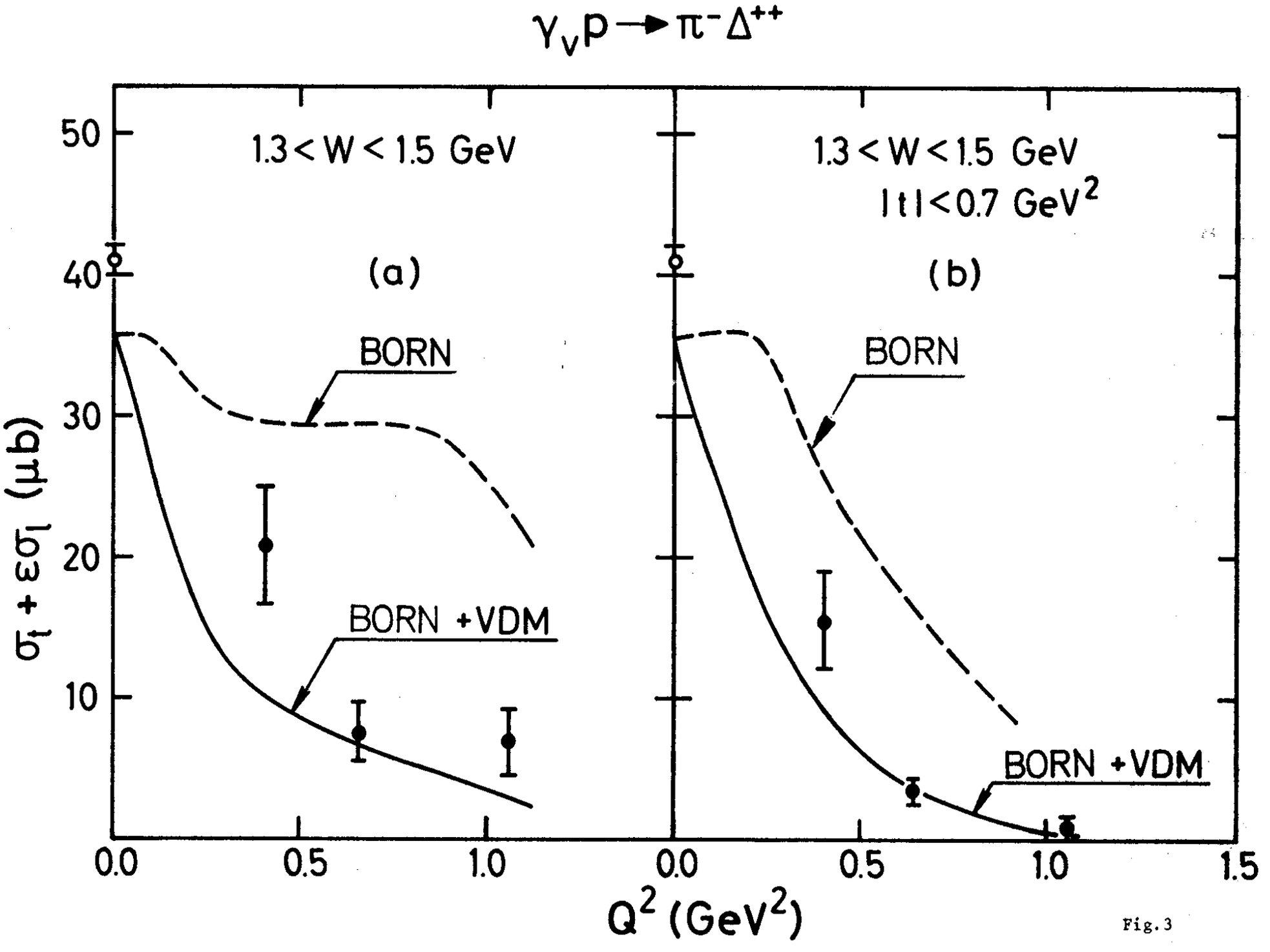
$\gamma_v p \rightarrow \pi^- \Delta^{++}$
1.3 < W < 1.5 GeV
(a)
BORN
BORN +VDM
1.3 < W < 1.5 GeV
|t| < 0.7 GeV^2
(b)
BORN
BORN +VDM
$\sigma_t + \varepsilon\sigma_l$ (μb)
Q^2 (GeV^2)
50
40
30
20
10
0.0
0.5
1.0
0.0
0.5
1.0
1.5

Fig.3

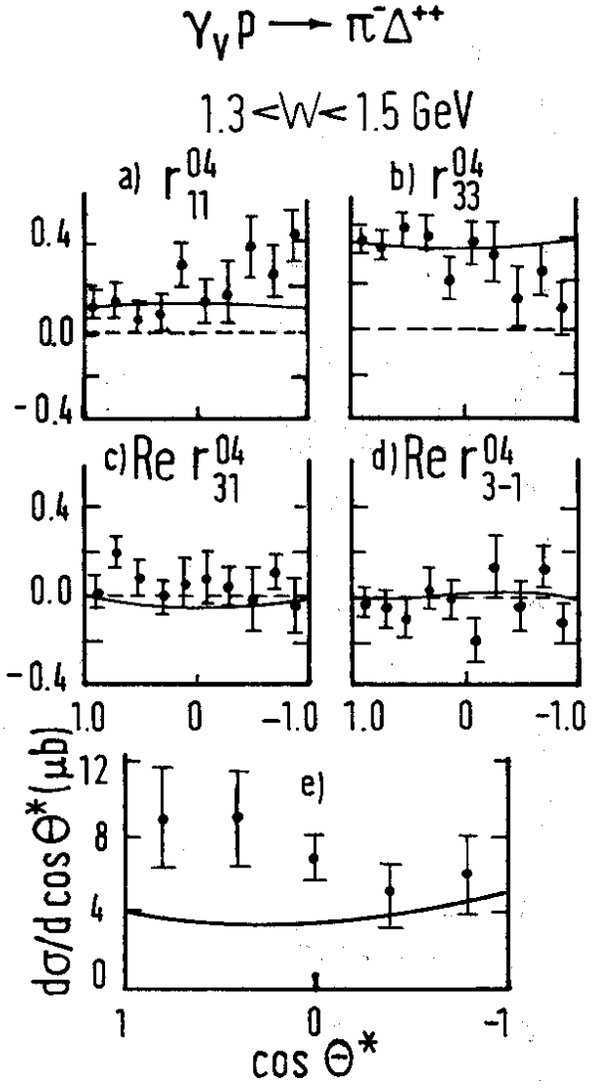
$\gamma_V p \rightarrow \pi^- \Delta^{++}$
1.3<W<1.5 GeV
a) r^{04}_{11}
b) r^{04}_{33}
c) Re r^{04}_{31}
d) Re r^{04}_{3-1}
0.4
0.0
-0.4
1.0
0
-1.0
e)
$d\sigma/d\cos\Theta^*(\mu b)$
12
8
4
0
1
0
-1
$\cos\Theta^*$

Fig.4

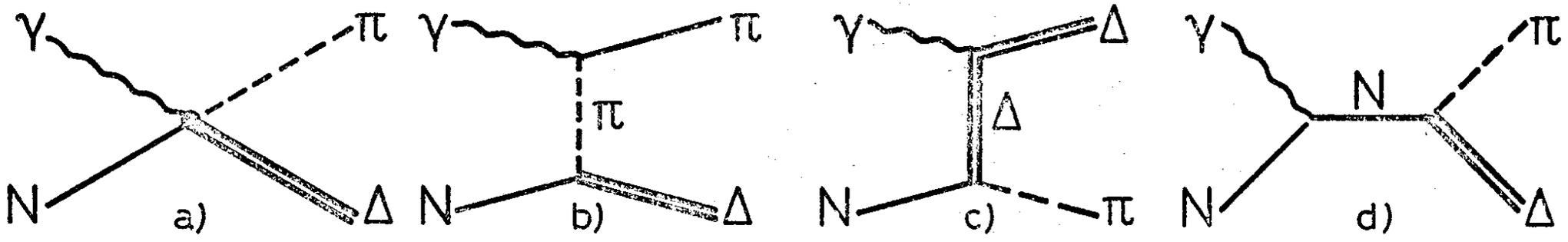

Fig.5